Supplement of SOIL, 12, 1079–1099, 2026
https://doi.org/10.5194/soil-12-1079-2026-supplement
© Author(s) 2026. CC BY 4.0 License.

Supplement of

Microbial carbon use efficiency emerges from interactions between soil structure and life-history strategies

Maëlle Maestrali et al.

Correspondence to: Maëlle Maestrali (maelle.maestrali@uni-hohenheim.de)

The copyright of individual parts of the supplement might differ from the article licence.

Supplementary figures: General simulations

Table S1 : Presentation of the different cellular states present in the simulations

Grid cell identity	Value in the state matrix	Immutable	Associated with resources
Soil solid phase	3	Yes	No
Air-filled porosity	30	Yes	No
Water-filled porosity	0	No	No
Resource	2	No	Yes
Motile r-strategist	1	No	Yes
Immobile r-strategist	4	No	Yes
Motile K-strategist	7	No	Yes
Immobile K-strategist	8	No	Yes

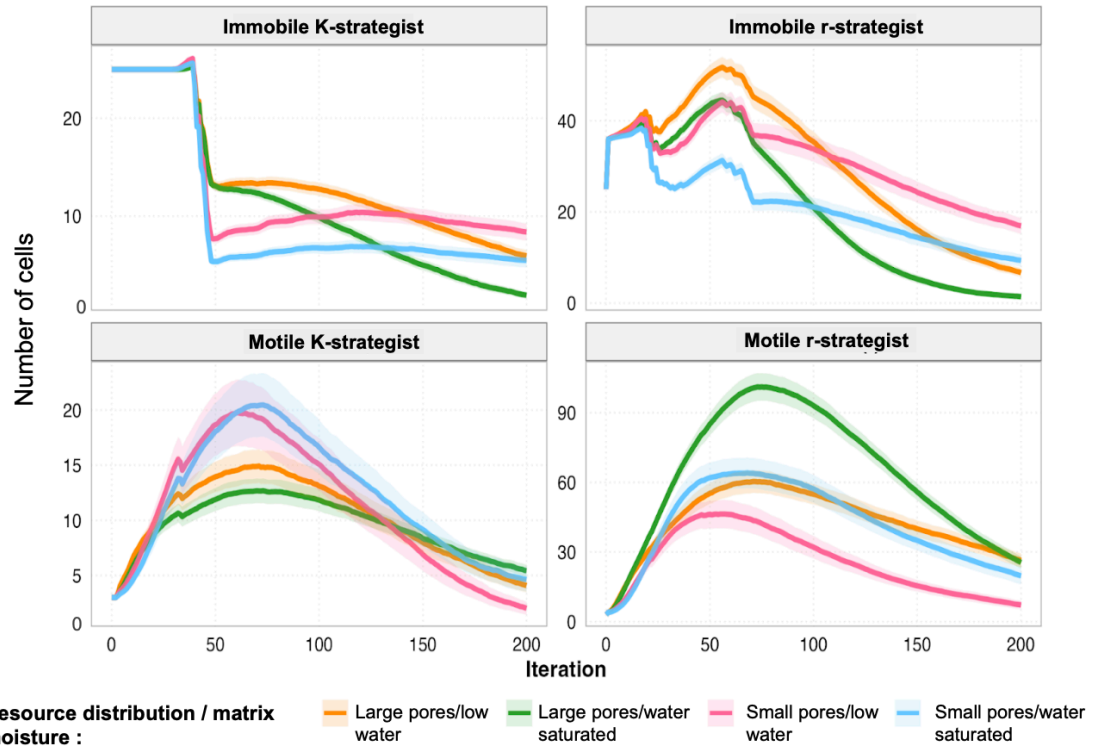


Figure S1 : Number of motile and immobile cells with either r- or K-strategies. Results for populations with 28 initial. The colors refer to the different initial matrix configurations, where, resources were distributed in the large pores (orange and green) or in the small pores (pink and blue). Matrices were either saturated with water (green and blue) or low water (pink and orange). For reasons of legibility, the scales used are different.

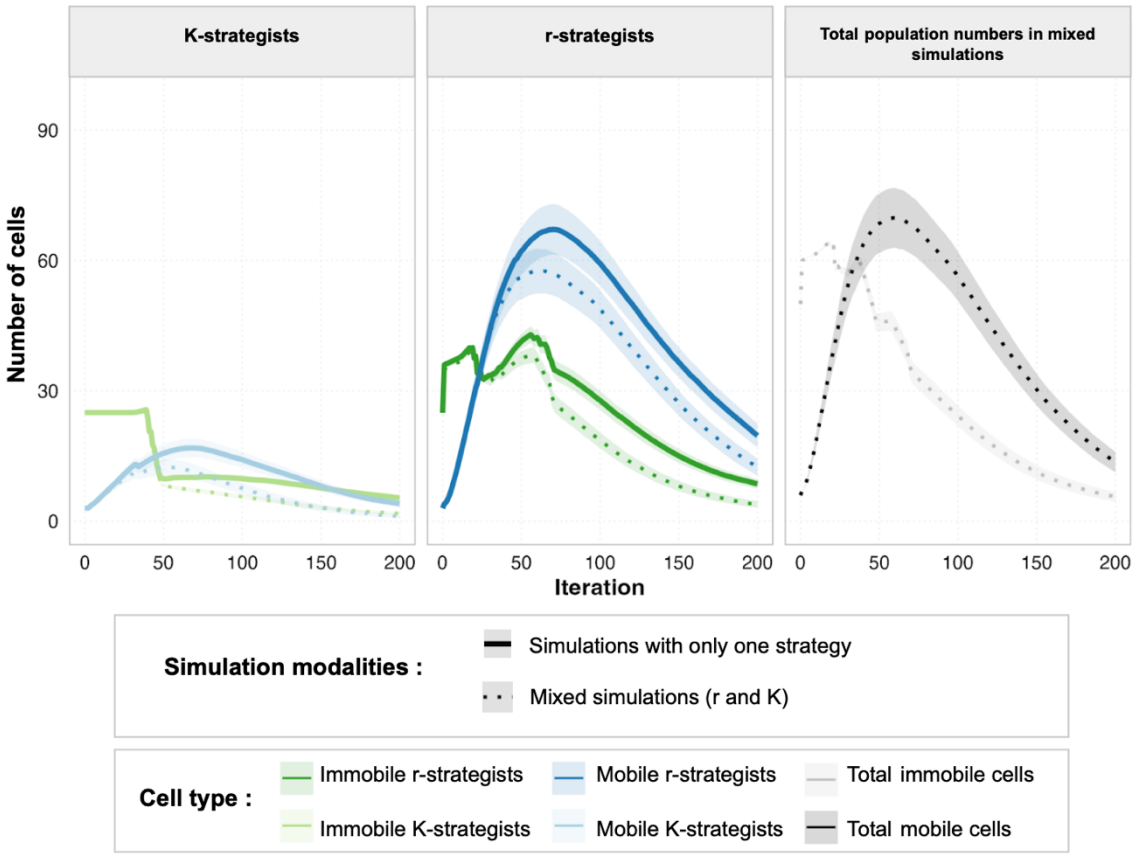


Figure S2: Graphical panel showing K-cell, r-cell and total cell populations for mixed simulations involving r-cells (56) and K-cells (56) in the same matrix. Solid lines refer to simulations without competition: K50_6 and r50_6 correspond to situations with K strategists only (50 immobile K cells and 6 motile K cells) and r strategists only (25 motile r cells and 3 immobile r cells) respectively. The dashed lines (rK25_3) show the results of simulations with competition, where r and K cells have been added jointly to the matrices. The grey curve in the third panel is the sum of the immobile K and r cells in the previous two panels. The black curve on the third facet is the sum of moving K and r cells on the previous two facets.

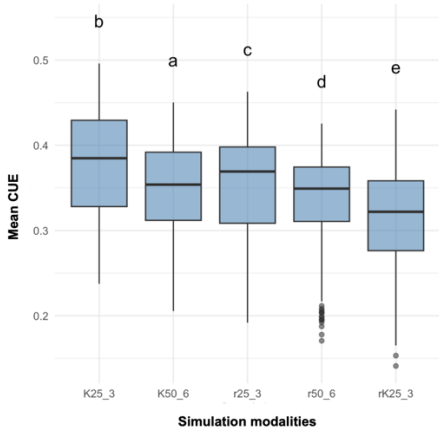


Figure S3: Box plot showing the effect of the simulation modalities on CUE. K25_3 and K50_6 correspond to situations with K strategists only (25 immobile K cells and 3 motile K cells or 50 motile K cells and 6 immobile K cells respectively). r25_3 and r50_6 correspond to situations with r strategists only (25 immobile r cells and 3 motile r cells or 50 motile r cells and 6 immobile r cells respectively). rK25_3 show the results of simulations with competition, where r and K cells have been added jointly to the matrices (25 immobile K cells and 3 motile K cells with 25 motile r cells and 3 immobile r cells). The letters correspond to the statistical groups given by a Tuckey analysis.

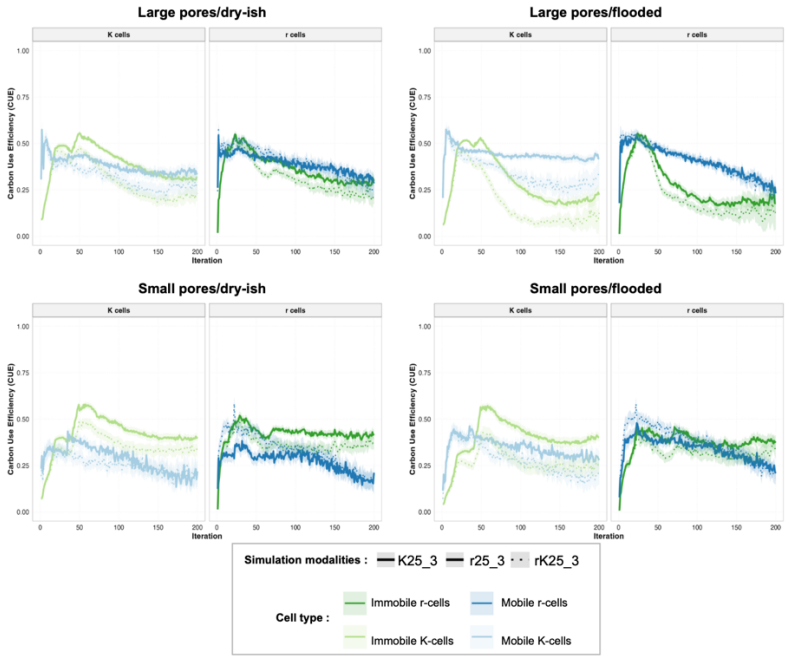


Figure S4 : Graphical panel showing the evolution of CUE over time in different initial matrix configurations, resources distributed in large pores or small pores with or without water saturation. Colors refer to the different cell types present in the matrices. Solid lines refer to simulations without competition: K25_3 and r25_3 correspond to situations with K strategists only (25 immobile K cells and 3 motile K cells) and r strategists only (25 motile r cells and 3 immobile r cells) respectively. The dashed lines show the results of simulations with competition, where r and K cells have been added jointly to the matrices.

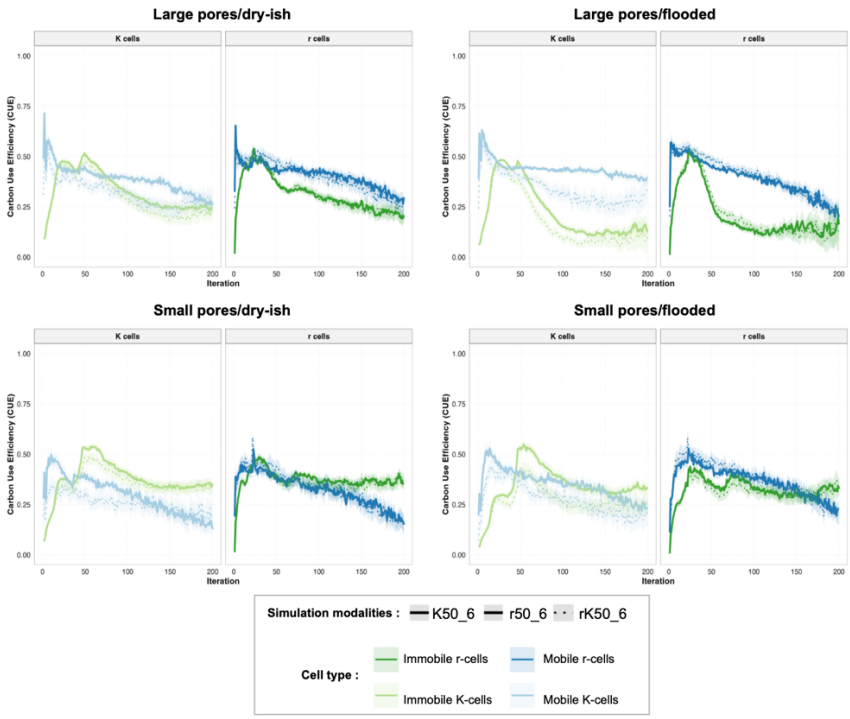


Figure S5 : Graphical panel showing the evolution of CUE over time in different initial matrix configurations, resources distributed in large pores or small pores with or without water saturation. Colors refer to the different cell types present in the matrices. Solid lines refer to simulations without competition: K25_3 and r25_3 correspond to situations with K strategists only (25 immobile K cells and 3 motile K cells) and r strategists only (25 motile r cells and 3

immobile r cells) respectively. The dashed lines show the results of simulations with competition, where r and K cells have been added jointly to the matrices.

Supplementary data: sensitivity tests

To determine the automaton sensitivity to the various model parameters, additional simulations were carried out. As for the main analysis, for each complementary simulation studied, 20 repetitions of 200 iterations were set up.

S1 Effect of moisture

Methods

To characterize the effect of different humidity levels on the development of r and K cells, a series of morphological expansions were applied to the solid elements of the matrix. For each level of dilation (parameter h varying from 0 to 15), the solid phase cells were dilated using a square kernel of increasing size (from 1 to 31 pixels). Newly expanded cells that were neither solid-phase cells nor resources were converted into water-filled pore cells (value 0 in the matrix), simulating progressive humidification of the system.

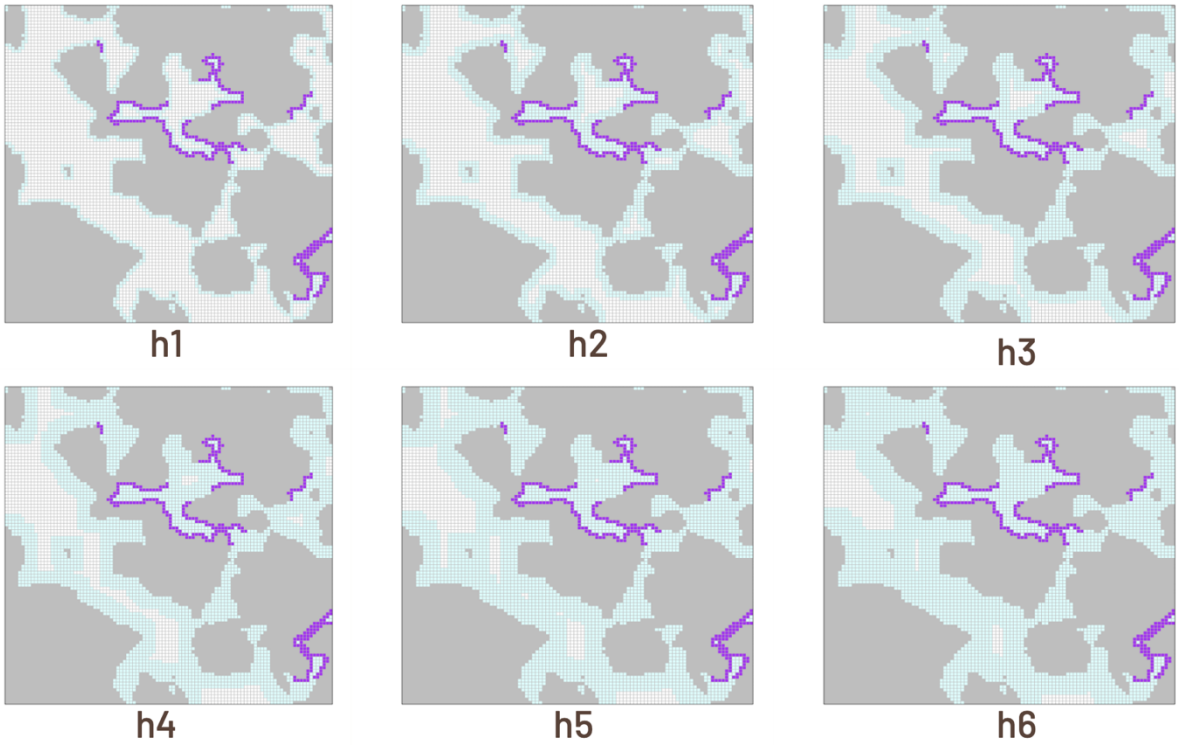


Figure S6: Images of 6 matrices used to test the model's sensitivity to the level of moisture. Matrix h1 is the least humid matrix (water film thickness covering solids and resources of 1 pixel), matrix h6 is a more humid matrix (water film thickness covering solids and resources of 6 pixels).

Results

Cell sensitivity to humidity only becomes apparent at the lowest humidity levels. Indeed, from a water film of 6 pixels, corresponding to a relatively high level of humidity, the smallest pores as well as a large proportion of the widest pores are nearly completely saturated with water, making differences between conditions less discernible. When resources are located in the largest pores, no significant effect of humidity was observed, either on motile or immobile cell populations, or on their carbon utilization efficiency (CUE). On the other hand, when resources are distributed in the smallest pores, humidity exerts a more marked influence. At the lowest moisture level (1 water film pixel), immobile cells had a higher average population (26.3 ±12.3) ($p < 0.001$) than motile cells (12.8 ±8.6). The CUE of immobile cells (0.41 ± 0.06) was also higher ($p < 0.001$) than that of motile cells (0.28 ± 0.12) at low humidity. This trend reversed at higher humidity levels, with a simultaneous increase ($p < 0.001$) in mean population (52.4 ± 23.6) and CUE (0.41 ± 0.10) associated with motile cells, and a decrease ($p < 0.001$) in mean population (16.3 ± 15.3) and CUE (0.20 ± 0.15) for immobile cells.

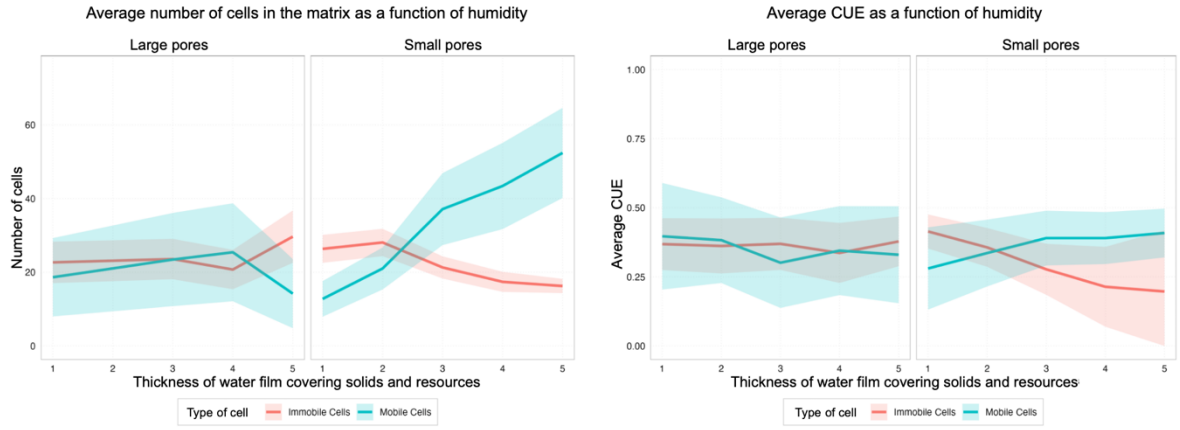


Figure S7: Graph showing the effect of water film thickness on the population and CUE of immobile and motile cells. Of the 15 moisture levels tested, only the top 5 are shown for both resource distribution pore sizes.

Discussion

The parameters selected for the main simulations appear relevant, insofar as they clearly distinguish between conditions with and without moisture constraints. Apart from extreme cases, the model seems relatively insensitive to fine variations in humidity levels, suggesting the existence of thresholds beyond which humidity is no longer a major limiting factor.

The results confirm that the main factors influencing motile cells are related to motility itself. These cells are particularly disadvantaged in restricted environments, characterized by narrow pores and low humidity, where the physical constraints on motility are increased. On the other hand, their performance improves markedly as humidity increases, facilitating their movement. Paradoxically, in high-humidity conditions, motile cells may be at an advantage when it comes to supplying resources to small pores, compared with distributions to larger pores, as resources diffuse less and are therefore more valuable when consumed.

Conversely, immobile cells are impacted by two types of constraints: (i) diffusive limitations linked to excessive humidity, which downgrades the nutritional value of resources, and (ii) exacerbated competition in environments more favorable to the proliferation of motile cells, which can reduce their access to resources. So, while immobile cells are less sensitive to variations in motility, they are more subject to the indirect effect of ecological dynamics induced by motile cells.

S2 Effect of resources concentration

Methods

To characterize the effect of initial resource concentration on the development of r- and K-type cell strategies, simulations were carried out by varying the concentration of resources available in the initial state. Eight levels of concentration were tested: 10, 25, 50, 75, 100, 150, 200 and 300 resource units of Resource per resource cell. The spatial distribution of resources was carried out in two modalities: either in large pores or in small pores. For each experimental condition, 20 repetitions were performed, each during 200 simulation iterations, using water-saturated matrices.

Results

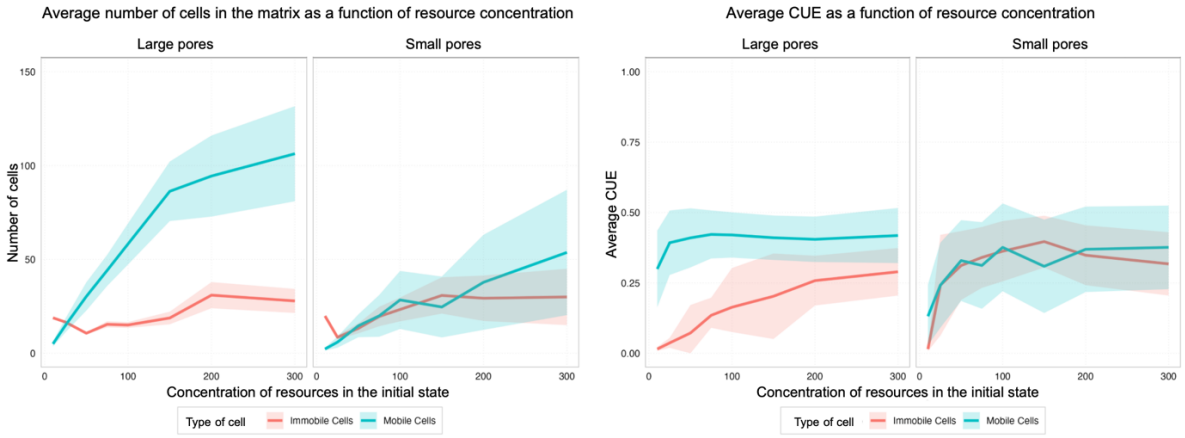


Figure S8: Graph showing the effect of resources concentration on the population and CUE of immobile and motile cells. 8 levels of concentration were tested 10, 25, 50, 75, 100, 150, 200 and 300 units of resource per resource cell.

In terms of cell number, when resource concentration is low (10 to 25 units of resource), resource consumption does not compensate for the benefits of movement for motile cells. Under these conditions, it is the immobile cells, with lower resource expenditure, that show better survival and higher average populations ($p<0.0001$). Generally, the increase in resource concentration is more favorable to motile cells, which will be able to move and consume more resources. In small pores, colonization dynamics remain limited, probably due to poor physical accessibility. However, once resources are diffused into these zones, their concentration remains high, which can compensate for the lack of motility and enable immobile cells to thrive. When resources are delivered to large pores, cell populations, particularly motile cells, appear to be less limited than in configurations where resources are located in small pores. A significantly higher capacity of motile cells to colonize the matrix is observed ($p<0.0001$).

For the carbon utilization efficiency (CUE), a stabilizing trend is observed above a certain resource concentration threshold. In configurations where resources are distributed in large pores, motile cells quickly reach their maximum CUE (0.38 ± 0.09), while the cue of immobile cells continues to grow with increasing resource con-

centration (from 0.02 ± 0.04 to 0.32 ± 0.07). When resources are localized in small pores, CUE dynamics are similar between motile and immobile cells, suggesting an attenuated effect of motility in these more constrained environments

Discussion

In our main simulations, we chose a concentration of 100 resource units per resource cell. This choice represents a compromise between two extremes: on the one hand, overly limiting conditions where resources become insufficient to allow the establishment of cell populations, and on the other, situations in which resources are so abundant that they no longer constitute a constraint, leading to excessive cell growth. The results obtained on the CUE confirm the relevance of this parameterization: at this concentration level, we observe differentiated and informative dynamics between motile and immobile cells, whose behavior is modulated by the size of the pores in which the resources are distributed.

S3 Effect of parameters governing living r and K cells

Methods

To study the effect of the different parameters modified between r and K cells in a more targeted way, complementary simulations were carried out by modifying the parameters of the K and r-strategist cells 1 by 1. The simulations performed can be considered as combinations of binary vectors of length 4, with two possibilities for each parameter: 0 or 1. In the case of the r strategy, all parameters are 'off' (0000), while for the K strategy, all parameters are 'on'. Between these two situations, we find all our intermediate mixtures, simulations S1 to S14 (1000, 1100, etc.). The simulations were carried out on a control matrix with a maximum moisture level and for both resource distributions, large pores and small pores.

Table S2 : Summary of the various simulations implemented and their associated costs

Simulation Id	Motility cost (m)	Maintenance cost (M)	Reproduction cost (r)	Reproduction threshold (R)
r strategist	*1*	*1*	*55*	*100*
S1	*1*	*1*	*55*	**250**
S2	*1*	*1*	**70**	*100*
S3	*1*	**3**	*55*	*100*
S4	**5**	*1*	*55*	*100*
S5	**5**	**3**	*55*	*100*
S6	**5**	*1*	**70**	100
S7	**5**	*1*	*55*	**250**
S8	*1*	**3**	**70**	*100*
S9	*1*	**3**	*55*	**250**
S10	*1*	*1*	**70**	**250**
S11	**5**	**3**	**70**	*100*

S12	**5**	*1*	**70**	**250**
S13	**5**	**3**	*55*	**250**
S14	*1*	**3**	**70**	**250**
K strategist	**5**	**3**	**70**	**250**

Results

Significant differences were detected in carbon use efficiency (CUE) between large-pore and small-pore conditions. The effect of pore size on CUE ($F=1149.13$; $p<0.001$) was greater than the individual effects of the life governing parameters, highlighting its strong influence on carbon use efficiency by microorganisms. It is important to note that pore size not only altered the overall CUE but also altered the combinations of parameters that maximised CUE. These optimal strategies varied considerably between large and narrow pores, and the differences were also modulated by cell motility, with motile and immobile cells exhibiting distinct combinations of parameters that yielded the best results in each pore condition.

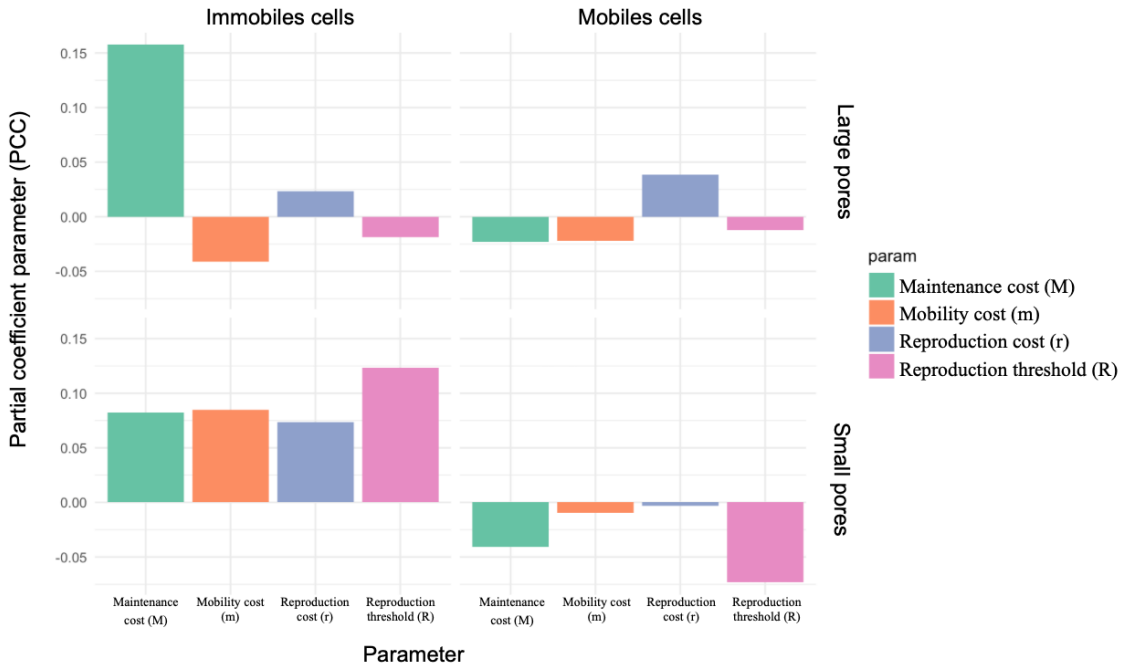


Figure S9 : Graphic panel showing the partial coefficients by rank for the four parameters studied, the effects are studied separately for each condition considered (pore x motility).

To assess the relative influence of the four experimental parameters (motility cost, maintenance cost, reproduction cost, and reproduction threshold) on CUE, we used partial correlation coefficients by rank (PCC) (Saltelli et al., 2000). The analysis was performed separately for each combination of pore size and motility to control for the effects of other parameters. For motile cells in large pores, none of the parameters showed a significant effect on output (PCC between −0.022 and 0.038), indicating low overall sensitivity. For immobile cells in large pores, maintenance cost appeared to be the most influential parameter (PCC = 0.158), while the other parameters had marginal effects.

In small pores, motile cells showed a weak negative correlation with maintenance cost (PCC = −0.041), with the other parameters having little influence. For immobile cells, the reproduction threshold had the most significant effect (PCC = 0.123), followed by the other parameters with moderate coefficients (0.074–0.085).

Overall, these results show that the sensitivity of the system depends heavily on cell type and porosity: immobile cells are more influenced by maintenance or reproduction threshold, while motile cells appear relatively insensitive to all parameters studied. These trends suggest that interventions targeting maintenance or reproduction threshold could have a differential impact depending on the cell type and environment considered.

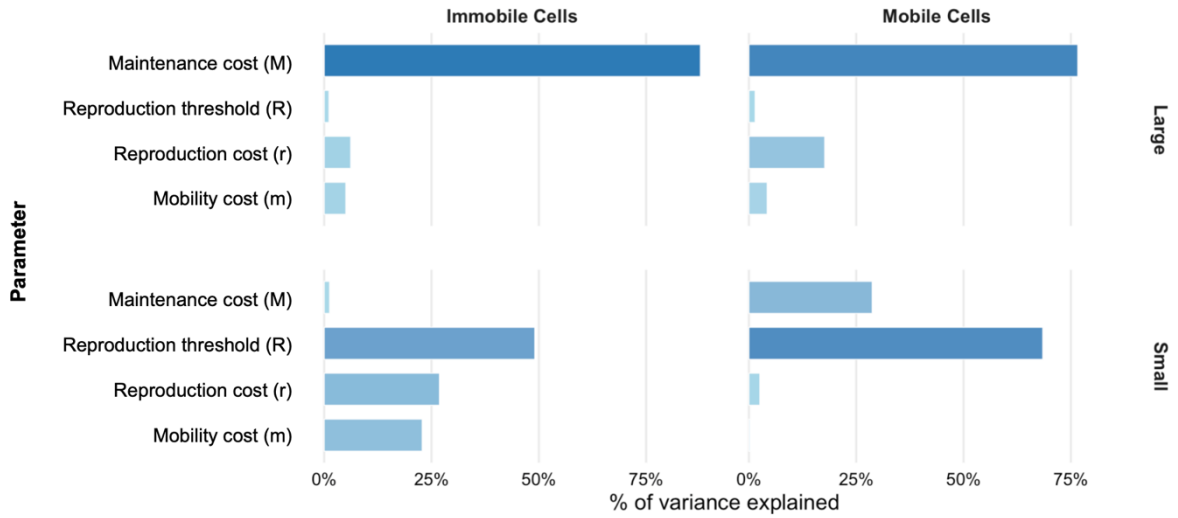


Figure S10: Explained variance for each parameter without considering any interactions. The intensity of the blue corresponds to the intensity of the parameter's effect. Given the significant interactions between the parameters, cell type (mobile/immobile) and pore size, the effects are studied separately for each condition considered.

In large pore environments, maintenance cost emerged as the dominant factor influencing CUE, explaining more than 70% of the variance for both motile and immobile cells. For motile cells, strategies with a lower maintenance cost consistently yielded higher CUE values. In contrast, for immobile cells, although the highest CUE was observed when the maintenance cost was at its maximum. The parameter combinations producing the highest CUE in large pores were m1_M1_r70_R100 **(S2)** for motile cells (CUE = 0.404 ± 0.099) and m1_M3_r70_R100 **(S8)** for immobile cells (mean CUE = 0.199 ± 0.154).

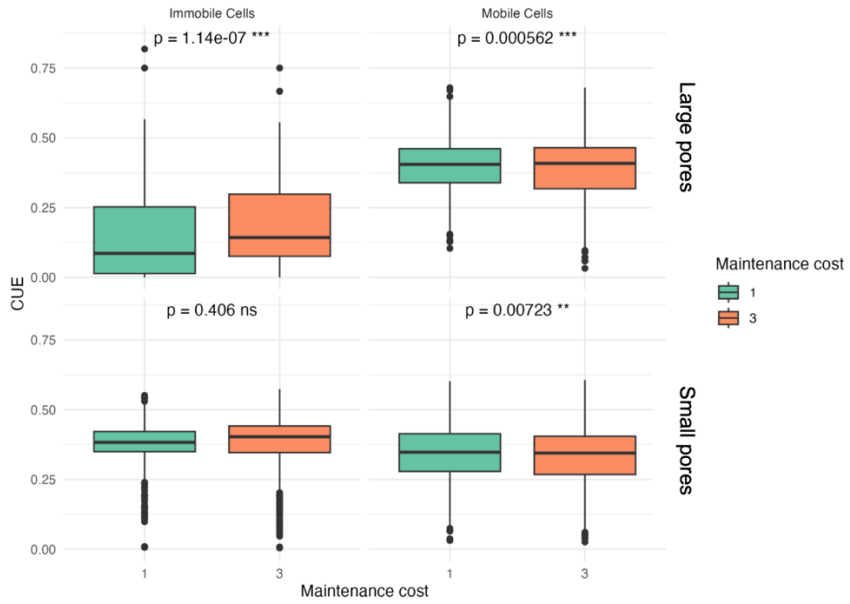


Figure S11: Distribution of CUE as a function of maintenance cost for different pore sizes (across rows) and different types of living cells (across columns). Maintenance cost is the individual parameter that best explains the observed variance in large pores.

In small pore environments, reproduction threshold emerged as the dominant factor influencing CUE, explaining more than 45% of the variance for both motile and immobile cells. For motile cells, strategies with a lower reproduction threshold (100) yielded higher CUE values. For immobile cells, the highest CUE was observed when the reproduction threshold was at its maximum (250). The parameter combinations producing the highest CUE in large pores were m1_M1_r55_R100 **(r complete)** for motile cells (CUE = 0.404 ± 0.099) and m5_M3_r55_R250 **(S13)** for immobile cells (mean CUE = 0.199 ± 0.154).

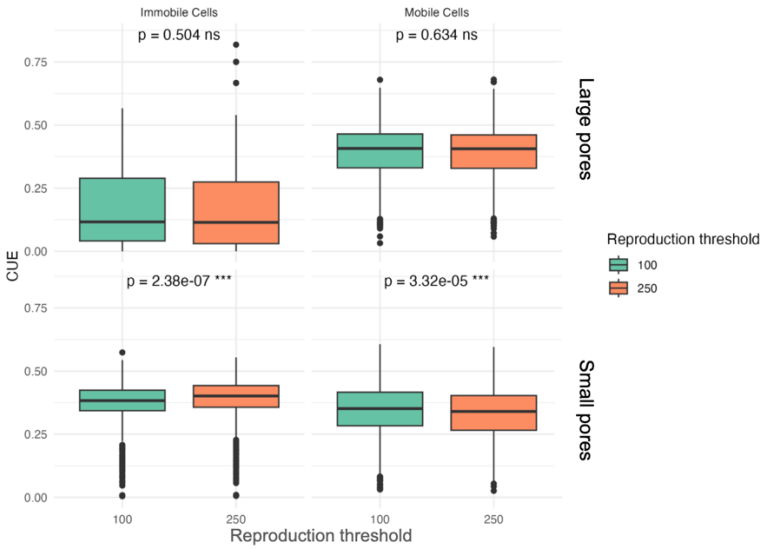


Figure S12 : Distribution of CUE as a function of reproduction threshold for different pore sizes (across rows) and different types of living cells (across columns). Reproduction threshold cost is the individual parameter that best explains the observed variance in large pores.

In the case of our simulations, we might expect strategies r (0000) and K (1111) to be the most different from each other and their effect on CUE to be the most opposite, thus resulting in a very negative or at least very weak correlation. However, analysis of the correlation matrices shows that the r and K simulations are never the most different, regardless of the type of living cell (mobile or immobile) or the pore size considered.

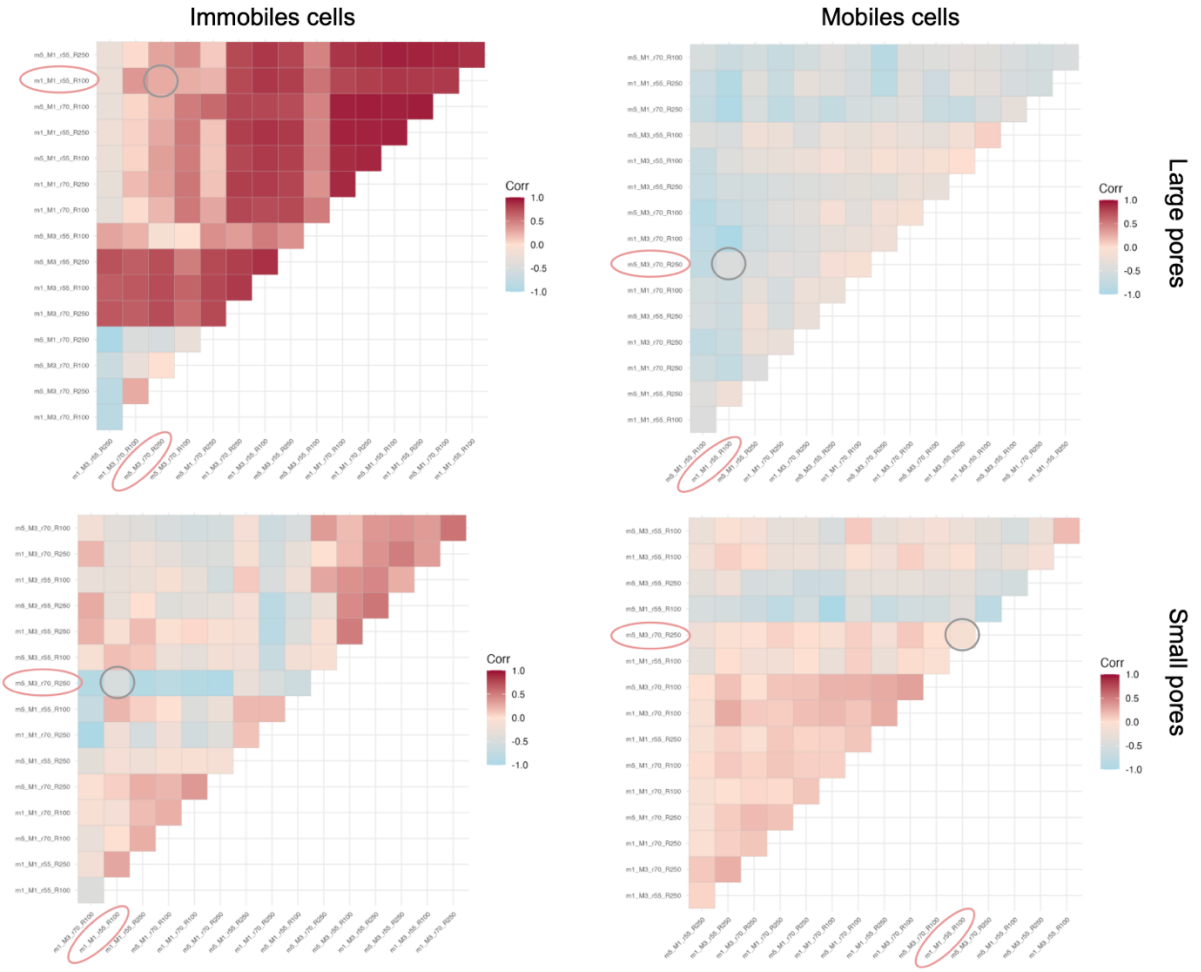


Figure S13 : Diagram showing the correlations between K and r simulations and those ranging from S1 to S14 for the different pore sizes and the two types of cells considered. The legends refer to the codes used in Supplementary Table 1, with m (motility cost), M (maintenance cost), r (reproduction cost) and R (reproduction threshold). The codes are followed by the associated resource point cost in the simulation, for example m1_M1_r55_R100 corresponds to the complete r simulation (motility cost = 1, maintenance cost = 1, reproduction cost = 55 and reproduction threshold = 100). The ellipses on the graph indicate the R and K strategies and their comparison.

This indicates that the effect of the parameters on CUE is not simply additive or independent. For example, certain partial combinations (S1, S2, etc.) can influence CUE more radically or unexpectedly than the direct transition from strategies r (0000) to K (1111). A Cramer analysis showed very low values (>0.01) for most parameter pairs, indicating a weak categorical association between parameters. There is one exception for the Immobile Cells group in large pores, where some values are slightly higher (0.03-0.05), but still low. This suggests that these parameters do not have strong redundancy or direct masking with each other; they appear to be relatively independent.

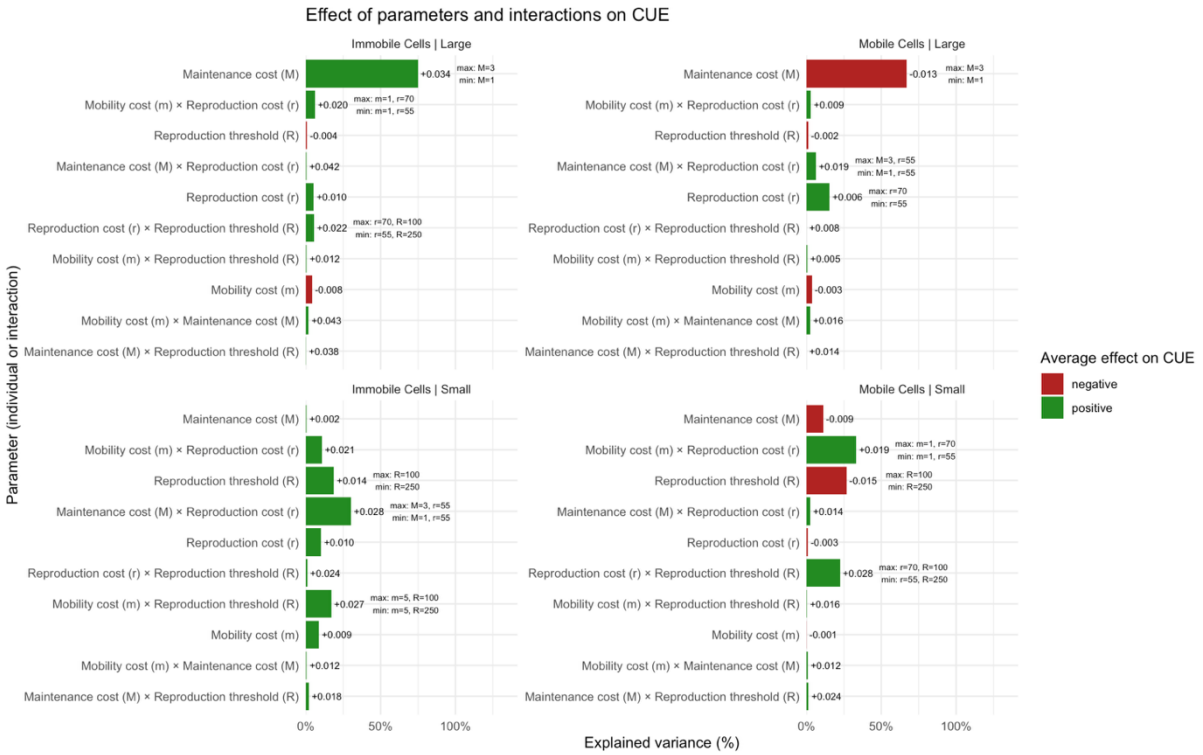


Figure S14: Correlogram showing, for each combination of cell type (Mobile Cells or Immobile Cells) and pore type (Gou P), the relative importance of individual parameters and their interactions in explaining the variance in CUE. Each bar corresponds to a term in the linear model, which can be a simple effect: a single parameter or an interaction between two parameters. The colour of the bars shows the average effect of the parameter on CUE. Green (positive effect): average increase in CUE when the parameter increases (or moves to a higher level). Red (negative effect): average decrease in CUE when the parameter increases. The numbers to the right of the bars refer to the average effect of the parameter on the CUE, calculated differently depending on the type of term. For simple effects, this is the average CUE difference between the two levels of the parameter (highest level minus lowest level). For interactions, it is the difference between the highest average and the lowest average among all possible combinations of the levels of the two parameters. These values are expressed directly in CUE units (for example, +0.034 indicates that the CUE increases by an average of 0.034 when the parameter changes from its low level to its high level). For the three parameters or combinations of parameters that best explain the variance, the parameter values that yield the maximum (max) and minimum (min) CUE are specified.

The significant effect of certain partial combinations of parameters (S1, S2, etc.) on the CUE can be explained by the presence of significant interaction effects. These interactions between the various parameters governing the life of living cells are modulated by the size of the pores and the type of cell considered. In the largest pores, interaction effects explain only a marginal part of the variance observed. In contrast, in small pores, interaction effects explain a larger part of the variance. Furthermore, the predominant interactions are not the same for all types of living cells studied. In the case of immobile cells, the interaction between the cost of maintenance and the cost of reproduction is the most important: the combination ‘maintenance cost = 3 and reproduction cost = 55’ maximizes the CUE, while a maintenance cost = 1 and reproduction cost = 55 gives a lower CUE. In the case of motile cells, it is the interaction between the cost of motility and the cost of reproduction that explains most of the variance, with maximum CUE observed when the cost of motility = 1 and the cost of reproduction = 70, and lower CUE when the cost of motility = 1 and the cost of reproduction = 55.

Discussion

Our goal was to conduct a targeted analysis of the parameters influencing the dynamics of r- and K-type cells. Here, we were able to highlight significant effects of the various parameters used in our simulations, as well as complex interaction effects, all modulated by pore size and the identity of living cells (mobile or immobile).

A notable finding is that, in most of the conditions tested, r-strategists exhibit the highest CUE values. However, this trend must be qualified: all simulations were performed in water-saturated pores, a condition that strongly influences cell response. Indeed, our simulations show that in dry pores, K-strategists frequently achieve the best performance.

Another important observation concerns the significance of the 'cost of motility', which may explain part of the variance even for immobile populations that do not incur this cost. This is because motile and immobile cells are present together in the matrices and their population dynamics are linked to each other, notably through competition. For example, a higher motility cost (=5) in the case of small pores can affect motile cell populations. In small pores, motility is less profitable than in large pores: the benefits that can be derived from it cannot compensate for an excessively high motility cost. Thus, in this situation, immobile cells can take advantage of the unfavorable situation for their motile counterparts and exhibit higher CUE values (+0.009).

Although we expected the r and K strategies to produce the most marked contrasts in terms of carbon use efficiency (CUE), our results show that it is not always the most 'opposite' strategies that generate the strongest differences. Pore size and the functional identity of the cells (mobile or immobile) also significantly modulated the responses observed. Furthermore, there was no universally optimal combination of parameters, nor is there any particularly deleterious configuration preventing the emergence of viable populations or significant CUE in the four simulated contexts. This complementary study suggests that while we chose to explore r and K strategies, other combinations of traits could represent less stereotypical but potentially relevant microbial ecological strategies. We chose r and K because they are well-established archetypes in ecology: the r strategy, focused on rapid and inexpensive reproduction, associated with low metabolic costs; and the K strategy, characterized by slow, costly reproduction and higher metabolic expenditure. These archetypes, widely described in the literature, are thought to be found in various soil environments (Li et al.). The results obtained in this complementary work show that rather than being limited to the classic opposition between r and K strategies, our model could be adapted to explore a three-dimensional framework inspired by Grime's RSE model, transposed to microbes in the form of the "YAS triangle " (Ho et al., 2013; Malik et al., 2020).

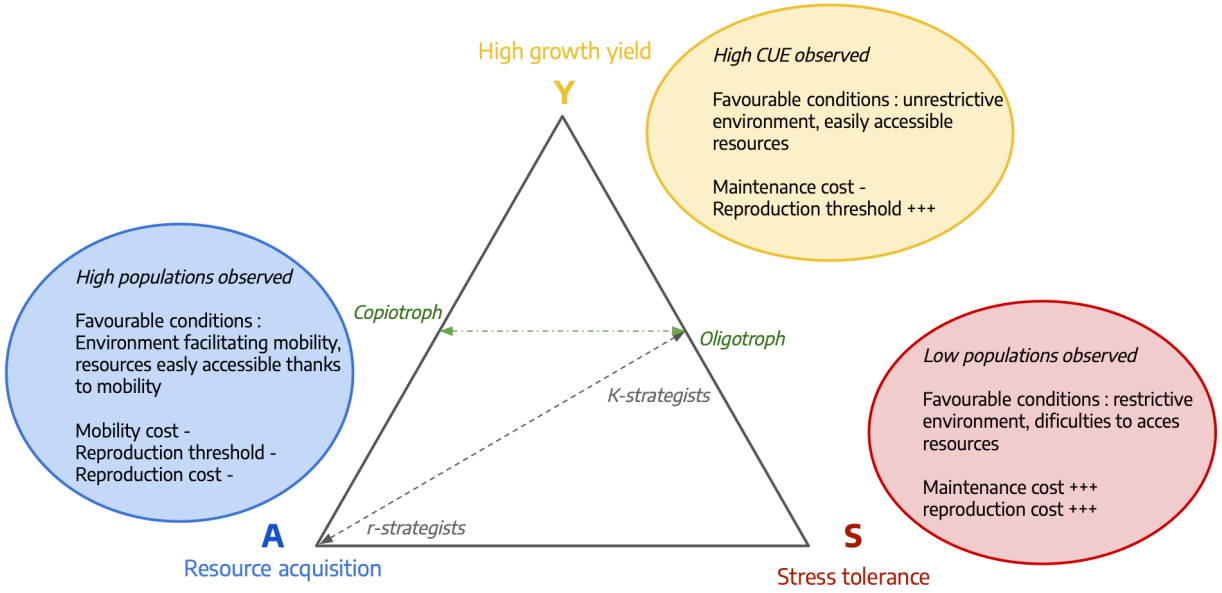


Figure S15 :Adaptation of the YAS triangle